International Journal of
INTELLIGENT SYSTEMS AND APPLICATIONS IN ENGINEERING
ISSN:2147-6799 www.ijisae.org Original Research Paper

Optimising Image-guided Needle Biopsy Procedures

[1]Doubt Simango*, [2]Tawanda Mushiri, [3]Abid Yahya, [4]Augustine Ndaimani

Submitted:13/03/2024 **Revised**: 28/04/2024 **Accepted**: 05/05/2024

Abstract: A minimally invasive technique called image-guided needle biopsy takes tissue samples for diagnosis or treatment. Needle biopsy operations can be carried out more precisely and accurately with surgical robotic arms than with manual techniques. However, controlling surgical robotic arms can be difficult because the patient's movements and any obstructions in the needle's route must be considered. Surgical robotic arms can be controlled more effectively using computer vision technologies when performing image-guided needle biopsy procedures. Using computer vision, real-time tracking of the needle tip location, detection and avoidance of obstructions in the needle's path, motion compensation for the patient, and instantaneous feedback to the surgeon regarding the procedure's success are all possible. Image cancer recognition and tracking system was developed using computer vision to extract cancer center coordinates from the computer vision pixel images. The significance of the suggested approach lies in its ability to raise the effectiveness and precision of surgical robotic arm control, allowing surgeons to execute a more extensive variety of procedures with more ease and precision. The study also includes the investigation of multi-modal imaging modalities, including CT, MRI, and ultrasound studies, leveraging computer vision to localize tissue and guide the needles precisely. The goal of creating a system that coordinates localization and segment brain tumors was achieved. The center coordinates of brain tumors have been extracted from CT scan pictures by effectively applying computer vision techniques. This resulted in increased procedure accuracy and precision, a lower risk of damaging blood vessels and nerves, better surgeon visualization of the procedure, and reduced number of needle insertions required. Overall, the safety and effectiveness of this crucial medical process could be raised by using computer vision to optimize the control of surgical robotic arms during image-guided needle biopsy procedures.

Keywords: *Image-guided needle biopsy, computer vision, surgical robotic arm, medical imaging*

1. Introduction

Robotic arms have recently turned around medicine through more precise diagnostic and therapeutic applications. The arms can be manipulated through mathematical models, PID control, forward and inverse kinematics, dynamics, or other control algorithms. Vision-based robotic arm control techniques incorporate computerized visual tracking and object recognition concepts [1,2]. Computer vision technology can allow robotic arms to operate without human interaction by employing cameras and algorithms to interpret visual input. Additionally, this technology may make more organic and intuitive control techniques like eye tracking and gesture recognition possible. Biopsy remains the gold standard in diagnosing most superficial and deep malignant neoplasms. While cutaneous biopsy can performed through shaving, punch, incisional, or excisional methods, biopsy for deep-seated neoplasms can be done through open surgery, endoscopy, or needle biopsy. Little bits of solid or liquid bodily tissue can be removed with a less invasive procedure called a percutaneous needle biopsy. Needles biopsy procedures have advanced in a number of ways in recent years, including precision biopsy using ultrasonic biopsy guidance and other imaging modalities such as CT, MRI, or X-ray biopsy guidance. Although computerized visual probes have been used in endoscopic biopsy operations, needle biopsy can also use them. This can facilitate needle injection into the required spot. For instance, computer vision can use coordinates to guide the trajectory of the needle during specimen collection. A sample from the desired area is taken to guide the biopsy needle and increase process accuracy. Precision medicine may benefit from the next generation of multimodal therapeutic approaches, which could help with the early identification of solid brain tumors and efficient treatment [3]. Pathologists benefit from computer-aided diagnosis (CAD), which develops numerous machine-learning and image-processing methods. This study examines the range of currently used computer-aided and manual breast cytology procedures [4]. Accurate cancer diagnosis and prognosis depend on ground breaking technological developments in molecular biology and cancer imaging [5]. The robots can also be used for non-operating room percutaneous biopsy, expanding the options for home-based diagnosis and therapy [6].Recent investigations have found that current surgical robotic systems for image-guided needle biopsies have an average trajectory variation of 2-3 millimeters from target sites. This deviation has been found to affect both patient outcomes and procedural accuracy.

[1] *Mechatronics Dept. Chinhoyi University of Technology*
ORCID ID: 0009-0005-6625-3232
[2, 4] *Biomedical Informatics. University of Zimbabwe*
ORCID ID: 000-0003-2562-2028
[3] *Botswana International University of Science and Technology. Botswana.,*
ORCID ID: 0000-0003-3741-8315
**corresponding Author Email:dsimango@cut.ac.zw*

Furthermore, clinical evaluations have revealed a 15-20% increase in procedural time in non-robotic-assisted procedures compared to standards, which might be attributable to inadequate decision assistance and feedback systems. Additionally, studies have shown that current constraints on feedback accuracy and response time are linked to a noteworthy 20% rise in procedure-related problems. These findings highlight the critical need for procedural precision and efficiency improvements by addressing constraints on response time, decision-making speed, and trajectory accuracy during robotically assisted needle biopsy operations. In light of this, combining computer vision technology with surgical robotic arms offers a ground-breaking chance to completely alter the field of minimally invasive procedures. By utilizing cutting-edge image analysis algorithms and multi-modal data fusion, image-guided needle biopsy operations might be made much more precise, safe, and practical, eventually improving patient outcomes and establishing new standards for procedural excellence. This paper aims to apply computer vision technologies to optimize the control of a robotic surgical arm. In particular, the study looks at how computer vision algorithms can monitor and recognize objects and how they can be integrated with control algorithms to operate the robotic arm actuators. Through tackling these obstacles, the goal is to create a surgical robotic arm control system that is more dependable and efficient, potentially finding use in the medical field.

1.1. The Comprehensive Theoretical Basis

An image-guided biopsy uses static or real-time imaging to guide the removal of a tissue sample from beneath the skin to offer diagnostic data [3]. The C-arm fluoroscopy technique uses a single X-ray image to calculate movement and assess aiming accuracy, which minimizes radiation exposure and operating time. The precision and reliability of the method have been assessed in pre-clinical studies and robot-assisted pedicle screw placement operations. Since the touch sense of surgical robots is still evolving, using a robotic system in the operating room is difficult. Robotic equipment was upgraded by employing newly developed intraoperative X-ray imaging technologies that facilitate lesion location to tackle the lesion location. [7]. Not only may robots be trained to perform repeated jobs, but their usage in ultrasound-guided percutaneous puncture also reduces operator fatigue. A multitude of robotic systems have been developed to facilitate ultrasound-guided biopsy procedures. According to [8], a novel robot-assisted method for transrectal ultrasound-guided prostate biopsy has been demonstrated in five clinical cases to be associated with very minimal distortion of the prostate, suggesting that it is safe and practical to use the robot to help with prostate biopsy. Additionally, robotic needle biopsy was demonstrated to be effective in targeting breast lesions identified through magnetic resonance imaging (MRI) using ultrasound guidance [9]. The use of ultrasonography in robotic needle biopsies is growing over time. As an example, a robotic device was evaluated on five puncture sites. It was found to reduce the number of needle insertions and increase accuracy compared to free-hand punctures [10]. Additionally, to optimize the image quality of an ultrasonogram, innovative robotic control methods for ultrasound imaging can use variable impedance control [11]. An additional option for the robotic system is to have two arms: an ultrasonic scanning arm and a puncture arm. These arms can be equipped with master-slave control and compliant positioning functions to improve the success rate of renal puncture surgery [12].Numerous MRI-guided robotic systems have been created to lower patient risk and improve intra-tumor probe placement accuracy. High-contrast images of the interior organs are obtained using magnetic resonance imaging (MRI), which combines radio waves, computer processing, and magnetic fields. By interpreting the MRI pictures, the surgical robots may be taught to insert the needle precisely, reducing the chance of errors or unintended consequences. Patient danger is typically increased by iterative positioning and imaging caused by inadequate physician grasp of patients in the MRI scanner. As a result, a strong teleoperated system and an instrumented testing platform were created and successfully used for robotic MRI-guided percutaneous and epicutaneous punctures. For malignancies like hepatocellular carcinoma, which is often treated with percutaneous ablation, MRI can also be used to guide ablative therapy. Determining the exact position of the intra-tumour probe is so crucial.

An MRI-guided percutaneous needle treatment using a semi-automated robotic system with concurrent MRI compatibility testing revealed that. A better technique to improve the MRI procedure and provide great visibility of the target lesion without ionizing radiation is to use end effectors aligned with the cancer target site under MRI guidance [13]. While the GUI software waits for the CT Scan Dataset to be received, CT scan images are imported The OpenCV thresholding algorithm executes on CT Scan images followed by morphological operations, contours are drawn to generate centroid coordinates, and GUI is linked to inverse kinematics execution for the surgical robot joints to execute the movement.

Even though it can be difficult, computed tomography (CT) guided needle insertion has been safely utilized to collect biopsy specimens and effectively proven in a swine kidney model [14]. Percutaneous needle insertion into common target organs such as the liver, kidneys, lungs, and retroperitoneum was successfully guided by a patient-mounted, CT-guided robotic system with five degrees of motion in a porcine model to assess the accuracy and precision of a robotic technique to perform robotics [15].To reduce the radiation the doctor is exposed to during the

procedure, a method for measuring the robot's angle offset using CT technology and a compensating technique was proposed. Their method's effectiveness was confirmed through experiments, and a surgery support robot called ZEROBOT was developed. They developed a robotic method guided by CT that can accurately position needles with an error of less than 2 mm [16].

A paper published investigated the application of haptic feedback to teleoperation tasks in a robotic arm system. The study showed how haptic feedback can enhance task performance and lessen user fatigue.

A low-cost embedded controller was suggested for building a bare structured pneumatic robot arm. The research aimed to create lightweight actuators for use in flexible robotic arms. The robot's motions are guided by the items it detects and tracks in its surroundings, which are detected and tracked using computer vision algorithms.

Analyze the image's edge gradient distribution to determine which areas are more likely to contain objects. However, they May have trouble with intricate backdrops or occlusions, may be sensitive to shifts in lighting or angle, and may be computationally costly for massive datasets or high-resolution photos.

In any background or terrain, the moving item may be detected and tracked by the algorithm analyzed from sources in a series of video frames captured by a stationary camera [17]. Deep learning (DL) is a burgeoning multidisciplinary field in its early stages. In the present era, DL designs can be successfully applied to challenges across a wide range of sectors due to the increasing availability of data [18]. To improve the SIFT algorithm's slow matching speed, this paper's suggested approach outperformed alternative algorithms in terms of efficiency, reduced algorithm error, and lowered the time required to process images [19].

[20] identified two primary categories of visual servoing: image-based visual servoing (IBVS) and position-based visual servoing (PBVS). In IBVS, the robot's mobility is controlled by the image features taken from the camera; in PBVS, on the other hand, the robot's motion is controlled by the orientation and location of the item being managed.

One visual servoing method is image-based visual servoing (IBVS), in which the robot's motion is managed using the camera's image features [21]. IBVS aims to regulate the robot's position and orientation in a closed-loop system by using visual feedback from the camera [22].

As per [22], position-based visual servoing (PBVS) is a kind of visual servoing technology in which the robot's motion is controlled according to its position and orientation concerning the object being manipulated. The objective of PBVS is to regulate the robot's position and orientation in a closed-loop system using the visual feedback obtained from the camera. While there are various methods for implementing PBVS, the fundamental concept is to estimate the object's position and orientation of the robot using the camera [21]. Overall, IBVS is a powerful technique for controlling the motion of a robot based on visual feedback and is used in various applications, including object tracking, pick-and-place tasks, and visual inspection [20].

2. Method

The authors defined the system requirements based on clinical needs to develop GUI software for extracting coordinates to guide surgical robotic arms. Initially, computer vision algorithms to identify biopsy targets and analyze medical images were developed using Python software. Then, image pre-processing through contouring algorithms, morphological procedures, thresholding, feature extraction, and target localization were done using Open CV in the Python 3.8 environment. Medical imaging datasets, such as CT scans or MRI images of brain cancer, were used for deep learning algorithm training and validation. Lastly, Python-based frameworks will validate the integrated system in virtual environments. Extensive testing was also conducted to ensure accurate localization and identification of biopsy targets on CT or MRI image scans for the precision of needle insertion. The machine-learning process is summarized in Figure 1. The end effector received an image of a contoured brain tumor with center positions represented in (x, y) coordinates.

2.1. System Flowchart

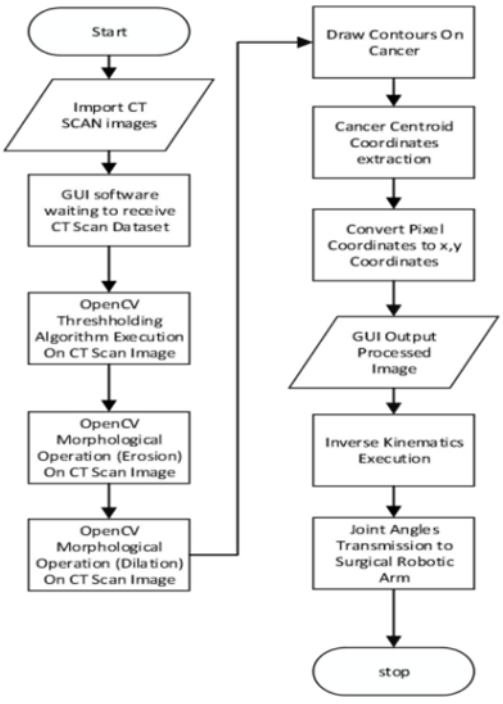

Fig 1. Flowchart for System Architecture.

RGB pictures showing healthy and cancerous brain images from the (Brain et al. for Brain Tumour Detection|

Kaggle.com, 2018) dataset created an image processing system for computer vision-based brain cancer recognition and diagnosis. The dataset comprises 253 images that were used for training and validations. Among these images, 98 were from normal head tissue, and 155 were abnormal.

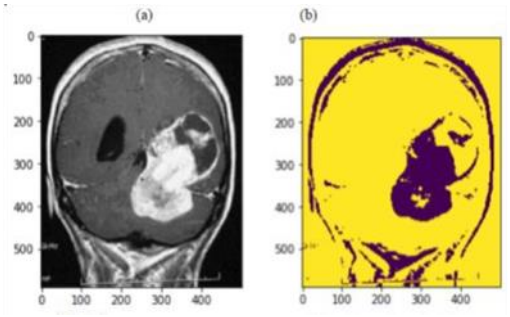

Fig 2. (a) Before Thresholding (b) After Thresholding.

Applying thresholding techniques to medical CT scans in the dataset makes it possible to isolate and highlight areas of abnormal tissue, potentially indicating the presence of tumors or cancerous growths, as shown in Fig. 5 above. This segmentation process aids medical professionals in precisely identifying and analyzing regions of interest, contributing to early tumor detection and treatment planning.

2.2. Image Contouring Model

The authors used the cv2.find Contours () function in OpenCV. This function takes three primary parameters:

1. image: The input image must be binary.

2. contours: An output vector that stores the objects' contours in the image.

3. hierarchy: An output vector that stores the hierarchy of the contours.

2.3. Testing of Contouring

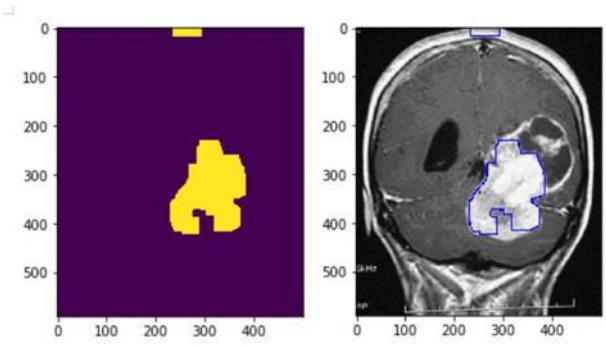

Fig 3. Contouring on Brain Cancer Cell on CT-Scan

These contours enable visualization of anatomical structures and serve as the basis for subsequent medical diagnostics and a safe biopsy procedure. Through OpenCV, the author discovered that contouring facilitates a crucial step in medical image analysis, assisting healthcare professionals in accurately delineating and characterizing anatomical features for diagnostic and treatment planning purposes.

2.4. Centre Coordinate Extraction after Contouring

After segmentation, the center of the lesion can be found by finding the centroid of the segmented lesion, as shown in Figure 4 below. The centroid of a region is the average of the x- and y-coordinates of all the pixels in the area of the contour. This is done by the equation below;

Let n be the number of points in the contour. The centroid (Cx, Cy) of the ith point (xi, yi) is calculated as follows:

$$c_x = \frac{1}{n}\sum_{i=0}^{n} x_1 \text{ and } c_y = \frac{1}{n}\sum_{i=0}^{n} y_i \quad (1)$$

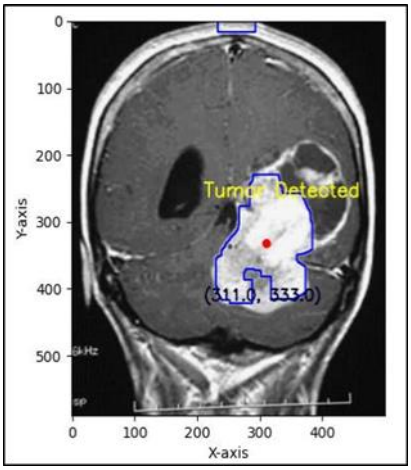

Fig 4. Extracting Brain Cancer Centre Coordinates

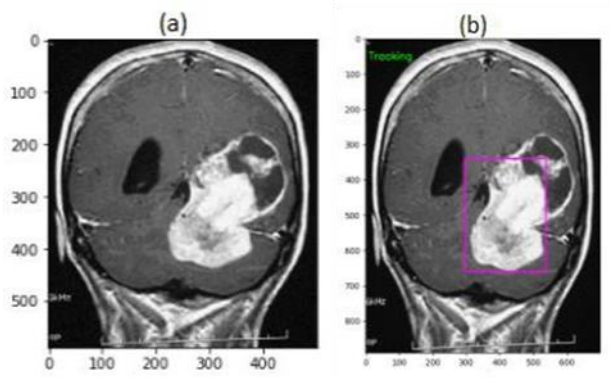

Fig 5. (a) Before Bounding (b) After Bounding

2.5. Centre Coordinate Extraction after Bounding

The center coordinates of a bounding box, as shown in Figure 9 below, can be obtained using the following formulas:

$$x\_center = x + (w / 2) \quad (2)$$

The Y coordinate of the center of the bounding box is calculated as the average of the Y coordinates of the top-left and bottom-left corners:

$$y\_center = y + (h / 2) \quad (3)$$

Where w and h are the width and height of the bounding box

The X coordinate of the center of the bounding box is calculated as the average of the X coordinates of the top-left and top-right corners. The author further uses the code above to draw the vertical line and horizontal line, which intersect at the center where:

(x, cy): defines the line's starting point at the top center of the bounding box.

(x + w, cy): defines the line's ending point at the bottom center of the bounding box

(0, 255, 0): specifies the color of the line as green. 2: represents the thickness of the line in pixels.

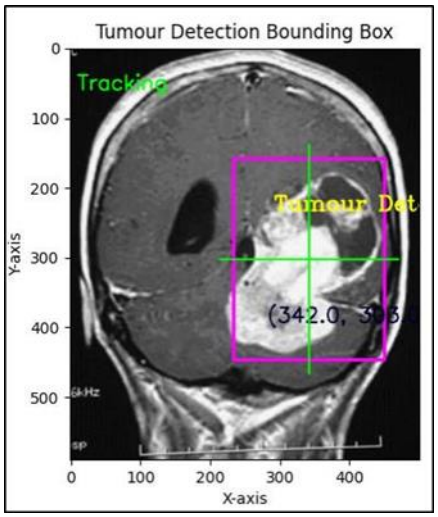

Fig 6. (a) Brain Cancer Centre Coordinates

2. Results and Discussion

Results using OpenCV Contouring and Bounding on CT-Scan Images

3.1. Training the Contouring and Bounding Model

The folder containing all the collected Dataset of all CT-Scan Images from (Brain et al. for Brain Tumor Detection| Kaggle.Com, 2018) Brain Tumour CT Scans is imported into the Contouring and Bounding Box model using the code.

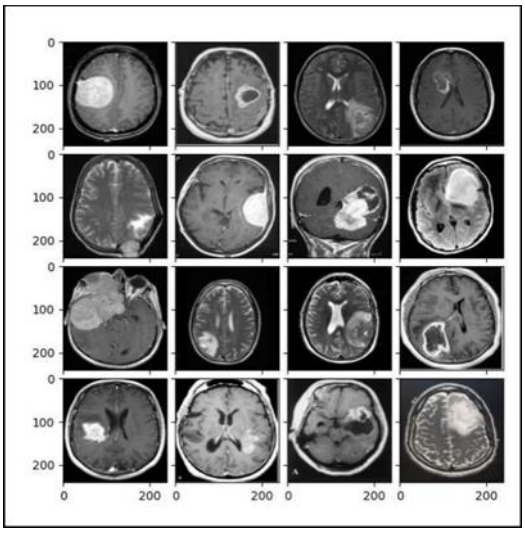

Fig 7. Output of Imported Images in the model

3.2. Results of Contouring and Bounding

Here, the author used Computer Vision contouring and bounding box OpenCV models using the same CT-Scan image in the dataset to locate the cancer in the brain. When utilizing the contouring model, the tumor's approximate center is indicated by a red dot in the center of the contour lines, painted in blue in the CT scan image. The operator is provided with a message, writing "tumor detected" in yellow, and the tumor's pixel coordinates (x, y) are also offered.

Similarly, the author employed the Bounding Box Model, indicating the approximate center coordinates of the tumor for its location in the CT scan image and drawing a bounding box around it in pink. A message is also provided to the operator, with "tumor detected" in yellow.

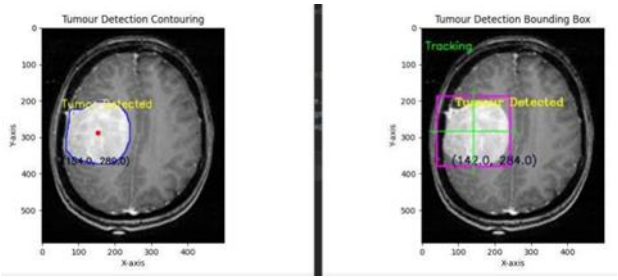

Fig 8. Contouring and Bounding Model on Brain Tumour

The author tested the center coordinate extraction using the models on other CT Scan images from the dataset, obtaining the center coordinates from contouring and bounding models.

3.3. Results of Contouring model on eight images bounding

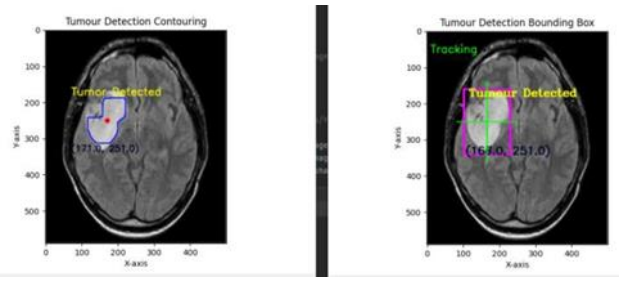

Fig 9. Y4 Image Scan Result

In this case, in fig. 9, the contouring model identifies 171.0 pixels of the tumor in image Y1, while the bounding box model identifies 163.0 pixels of the cancer in image Y1. This suggests that the bounding box model is less precise than the contouring model, capturing fewer pixels within the tumor. Both models agree that the center of the tumor is located at approximately (171.0 and 251.0) pixels on the image. This indicates a high degree of alignment between the two models regarding tumor localization.

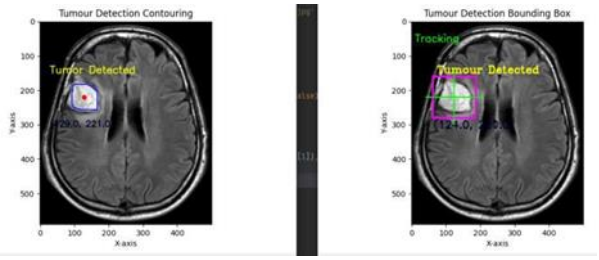

Fig 10. Y7 image scan Result

In this case, in Fig. 10, the contouring model identifies 129.0 pixels belonging to the tumor, while the bounding box model identifies 124.0 pixels. This indicates that the bounding box slightly underestimates the tumor's size compared to the contouring model. Both models agree that the tumor's center is located at approximately (129.0 and 221.0) pixels. This suggests a high degree of alignment between the two models regarding tumor localization.

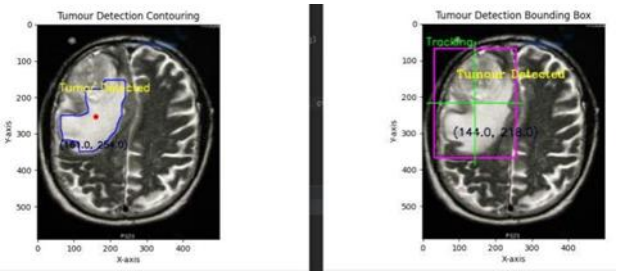

Fig 11. Y22 Image Scan Result

The bounding box model identifies 144.0 pixels, and the contouring model identifies more than in the tumor. This suggests that the bounding box significantly underestimates the tumor size compared to the contouring model. The contouring model and the bounding box model do not agree upon the center of the tumor, which places it at roughly (161.0, 254.0) and (144.0, 218.0) pixels, respectively. Given the substantial variation, this indicates a considerable difference in the perceived center point of the tumor between the two models. The cause is that the Y22 image represents a tumor with a complex shape, potentially explaining

the discrepancies between the contouring and bounding box models. The reason is that the tumor is located near the edge of the image, potentially influencing the bounding box model's accuracy in capturing its size and center.

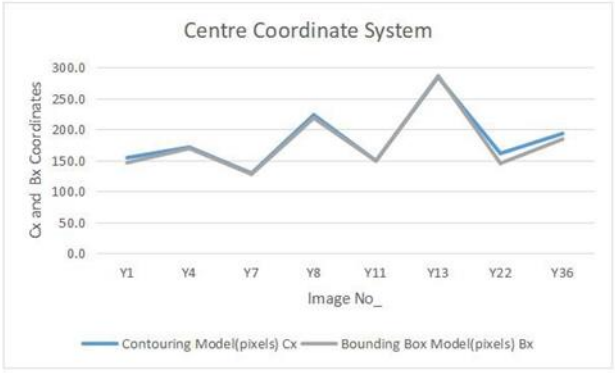

Fig 12. Chart Showing Contouring (Cx) coordinates and Bounding Box (Bx) coordinates

Fig. 12 shows the x coordinates of the contouring and bounding box models captured on different CT Scan images within the dataset. Regarding Accuracy, the Contouring Model generally provides more accurate x-coordinates for objects with complex shapes or irregular boundaries. Tracing the tumor's contour can capture intricate details and determine the center more precisely. Regarding Suitability, the Contouring Model is well-suited for applications where precise x-coordinate extraction is crucial, such as tumor tracking, precise tumor localization, and detailed image analysis.

The author ended up recording the center coordinates of each model on a table, as shown in Table 1 below, and the graphs were plotted below in fig. 13:

Table 1. Showing Contouring Model and Bounding Box Model Centre Coordinates

Image_No	Contouring Model(pixels)		Bounding Box Model(pixels)	
	Cx	Cy	Bx	By
Y1	154	289	146	289
Y4	171	251	163	254
Y7	129	221	124	220
Y8	223	246	218	235.5
Y11	149	306	149	308
Y13	284	127	286	134

Y22	161	254	144	218
Y36	193	220	184	251

Table 2. Interpretation of Cx and Bx Coordinates of both models

Image_No	Cx	Bx	Interpretation
Y1	154	146	Both models agree on the object's x-coordinate center, indicating high alignment.
Y4	171	163	Like Y1, both models are closely aligned in their center point estimation.
Y7	129	127.5	The difference between Cx and Bx is minimal, suggesting good model agreement.
Y8	223	218	Despite a slight discrepancy, the center estimations are still reasonably aligned.
Y11	149	149	Perfect match between Cx and Bx, demonstrating excellent agreement in object localization.
Y13	284	286	Another instance of perfect alignment between the two models' center point estimations.
Y22	161	145	The discrepancy between Cx and Bx is more significant than in previous cases, indicating potential inaccuracy in the bounding box model's center estimation.
Y36	193	184	Similar to Y22, the difference between Cx and Bx suggests inaccuracies in the bounding box model's center point detection.

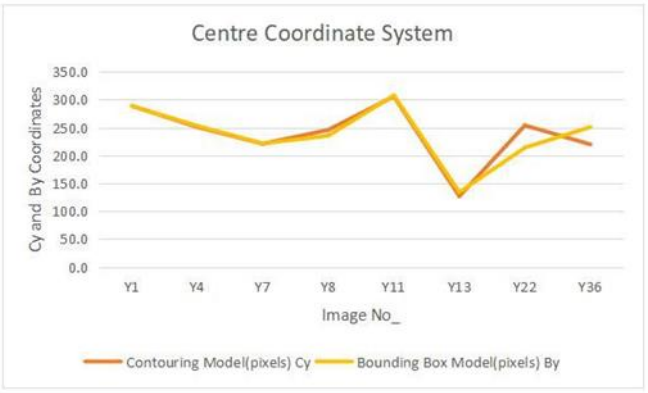

Fig 13. Chart Showing Contouring (Cy) coordinates, and Bounding Box (By) coordinates

Fig. 13 shows the x coordinates of the contouring and bounding box models captured on different CT Scan images within the dataset. Regarding Accuracy, the Bounding Box Model may be less accurate for objects with complex shapes or irregular boundaries. Since it uses a rectangular bounding box, it may not tightly enclose the tumor, resulting in less precise y-coordinates

Table 3. Interpretation of Cy and By Coordinates of both models

Image_No	Cy	By	Intertumor
Y1	289	289	Both models perfectly align in their Cy value, indicating excellent agreement.
Y4	251	254	There is minimal difference between Cy and By, suggesting good alignment.

Y7	221	218	There is a slight discrepancy, but overall, there is a good agreement in object center estimation.
Y8	246	235.5	Cy and By differ more than in previous examples, indicating potential inaccuracy in the bounding box model.
Y11	306	308	It is a perfect tumor boundary and calculates center coordinates for the tumor.
Y13	127	134	There is a minimal deviation between Cy and By, suggesting good agreement.
Y22	254	218	There is a significant difference between Cy and By, indicating substantial inaccuracy in the bounding box model for this image.
Y36	220	251	There is a large discrepancy between Cy and By, suggesting potential limitations in the bounding box model's performance.

The Bounding Box Model is more suitable for applications where a rough estimate of the y-coordinate is acceptable, such as tumor detection, approximate tumor localization, and quick image analysis. The author suggested that the Contouring Model is generally more accurate for complex objects and less sensitive to tumor rotation and perspective distortions. However, the Bounding Box Model is computationally more efficient and may be sufficient for applications where a rough estimate of the center coordinates is acceptable.

Inverse kinematics can be applied to the (x, y) pixel coordinates from computer vision to optimize control of a surgical robotic arm during image-guided needle biopsy procedures. It will serve as the center's standard for the end effector using the needle to remove the tumor. Consequently, the end effector's primary path would arrive at this location to support the surgeons doing a biopsy procedure.

3.1. Discussion

This study aimed to design a computer vision-based system to assist with image-guided needle biopsy procedures by optimizing the control of a surgical robotic arm. Specifically, the aims were to detect, segment, and locate brain tumours in CT scan images for coordinate extraction.

Both academics and industry have acknowledged the use of AI in healthcare in the revolution of robotics and health [24]. For this practice guideline, a proven, safe, and efficient method for a subset of patients with suspected pathology is image-guided percutaneous needle biopsy (PNB) [25]. For appropriate decision-making, including treatment planning, an image-guided needle biopsy is a safe and reliable non-surgical technique to diagnose suspected abnormal findings at breast imaging [26].Clinicians can identify and stage patients to select the best course of oncologic therapy using various innovative imaging technologies [27]. An image-guided percutaneous biopsy is a standard method in oncology, essential to tumor histology determination, cancer staging, and confirmation of the diagnosis [28]. Image-guided musculoskeletal (MSK) biopsies are a safe and efficient technique that can produce a diagnostic accuracy of up to 97% [29].

Many years ago, the concept of using robots for surgery was conceived, and soon after, a market need was established [30]. Because robotics improves accuracy and precision, even when percutaneous procedures are relatively basic, the quality of the process is significantly increased [31].

A critical first step in early detection is a timely and accurate tissue diagnosis. For experienced breast imagers, image-guided core needle breast biopsies are usually a straightforward process, although some common scenarios present special challenges [32]. An image-guided lung biopsy is necessary to detect and treat lung lesions [33]. The most recent advancements in actuation, sensors, novel materials, interventional devices, interactive/real-time MRI, and MRI-guided robot intervention are all thoroughly reviewed in this study. Novel clinical advances and future directions for study are also presented [34]. The microsurgery robot (MSR) has been the subject of extensive research over the last three decades because it can improve surgeons' operational skills through various jobs [35]. Medical imaging navigation technology is essential to intraoperative assisted puncture, preoperative robotic puncture path design, and surgical efficacy assessment. Robotic microneedle puncture has become a global research

hotspot [34]. In most organ systems, percutaneous needle biopsy (PNB) has a strong track record of safety, efficacy, and favorable results with minimal adverse effect rates. These treatments depend on imaging guidance, which enables the safe insertion of a needle into an organ or lesion to remove tissue for analysis [36].

The employment of surgical robots and image guidance has grown in percutaneous treatments to help reach internal organs or tissue through the skin; nevertheless, the advantages and disadvantages of these technologies have not been thoroughly investigated [37].Compared to traditional manual procedures, percutaneous puncture assisted by a surgical robot using image guidance has shown to be more accurate and efficient. It also puts less physical strain on the operator and decreases the chance of problems. Advanced imaging modalities, such as CT, MRI, and ultrasound, can provide accurate, high-resolution pictures to diagnose and treat various ailments, according to [37]. The benefits of the image-guided prostate biopsy robot include a high level of automation, independence from operator expertise and experience, decreased workload and operating time for urologists, and more. t makes up for the drawbacks of conventional free-hand biopsy and increases the precision and reliability of biopsy by delivering biopsy needles to predetermined biopsy areas with minimum needle placement errors [38].

One of the most significant developments in breast surgery over the past 20 years has been the ability to use vacuum-assisted, stereotactic, and percutaneous core needle biopsy (CNB) techniques to diagnose breast cancer outside of the operating room [39].Using a robotic arm, the suggested method locates the breast, identifies the target, captures and reconstructs the 3D ultrasound volume, and guides the needle. The EE thus features a stereo camera system, a needle stop, a pico-beamer, a US probe holder, and a three-DOF needle guide [40]. An all-in-one system that helps the radiologist with breast cancer imaging and biopsy was demonstrated. It is coupled to a robotic arm. Although the radiologist maintains control, like in the traditional approach, it has a high accuracy of needle placement [40]. Examining the precision of robot-assisted needle biopsy for skull base tumors was the main goal of the outcome measure. The five degrees of freedom robot used optical navigation to automatically inject a 14-gauge needle into the intended target [41].

Robotic technology is used to help surgeons during surgeries in a novel, cross-disciplinary research area called surgical robot systems (SRS). The inability to interpret complicated information and quick surgical judgments are examples of current SRS bottlenecks that have not been successfully resolved [42]. Surgical robots are comprehensive medical devices that, by replacing manual tasks with precision control, can reduce the risk of infection and trauma to patients after incisions. They incorporate numerous high-tech elements and symbolize interdisciplinary knowledge [43].

Image guiding is a common method for less invasive operations. Depending on the type of intervention, various imaging modalities are available. Common imaging modalities include computed tomography, magnetic resonance, and ultrasound [44].

Several studies present a unique, fully automated robotic-assisted system for positioning and inserting commercial full-core biopsy equipment under ultrasonography guidance, with its control and experimental evaluation [45]. To accomplish this, the authors created a cutting-edge robotic system that can identify the port and automatically position the scope in the best possible way [46].

Percutaneous needle biopsy (PNB) has been well-documented for its safety and effectiveness in most organ systems, with good outcomes and low rates of side effects. Imaging guidance, which permits the safe insertion of a needle into an organ or lesion to remove tissue for analysis, is crucial to these treatments [36].

The employment of surgical robots and image guidance has grown in percutaneous treatments to help reach internal organs or tissue through the skin; nevertheless, the advantages and disadvantages of these technologies have not been thoroughly investigated [37]. Percutaneous puncture assisted by a surgical robot with image guidance has proven more accurate and efficient than conventional manual operations. It also has a lower risk of complications and less physical strain on the operator. According to [37], advanced imaging modalities, including ultrasound, CT, and MRI, can produce precise, high-resolution images to help diagnose and treat various illnesses.

The benefits of the image-guided prostate biopsy robot include a high level of automation, independence from operator expertise and experience, decreased workload and operating time for urologists, and more. It makes up for the drawbacks of conventional free-hand biopsy. It increases the precision and reliability of biopsy by delivering biopsy needles to pre-defined biopsy areas with low needle placement errors [38].One of the most significant developments in breast surgery over the past 20 years has been the ability to use vacuum-assisted, stereotactic, and percutaneous core needle biopsy (CNB) techniques to diagnose breast cancer outside of the operating room (Klimberg & Rivere, 2016). The proposed approach involves the localization of the breast, target identification, 3D US volume capture and reconstruction, and needle guidance, all carried out by a robotic arm. As a result, the EE has a three-DOF needle guide, a needle stop, a picobeamer, a US probe holder, and a stereo camera system [40].

An all-in-one system that helps the radiologist with breast cancer imaging and biopsy was demonstrated. It is coupled to a robotic arm. Although the radiologist maintains control, like in the traditional approach, it has a high accuracy of needle placement [40]. Examining the precision of robot-assisted needle biopsy for skull base tumors was the main goal of the outcome measure. The robot with five degrees of freedom used optical navigation to automatically inject a 14-gauge needle into the intended target [41].

Robotic technology is used to help surgeons during surgeries in a novel, cross-disciplinary research area called surgical robot systems (SRS). The inability to interpret complicated information and quick surgical judgments are examples of current SRS bottlenecks that have not been successfully resolved [42]. Surgical robots are comprehensive medical devices that, by replacing manual tasks with precision control, can reduce the risk of infection and trauma to patients after incisions. They incorporate numerous high-tech elements and symbolize interdisciplinary knowledge [43].

A common method for less invasive operations is image guiding. Various imaging modalities are available, depending on the type of intervention. Common imaging modalities include computed tomography, magnetic resonance tomography, and ultrasound [44].A novel completely automated robotically assisted system with control and experimental assessment is presented in multiple publications [45] for the positioning and insertion of commercial full-core biopsy equipment under ultrasonography guidance. The authors developed a state-of-the-art robotic system that can recognize the port and autonomously place the scope in the most advantageous location to achieve this [46].

3. Conclusion

To achieve the objectives, the author explored various computer vision techniques using OpenCV in Python. Through processing functions like thresholding, morphological operations, and contouring, tumors could be isolated and highlighted from background tissue in CT scans. This image preprocessing allowed for the identification and tracking of potential biopsy targets.

The contouring model could precisely trace tumor boundaries and calculate center coordinates for tumor localization. Testing on sample CT images successfully located examples of brain cancer, with minimal discrepancies between the contouring model and bounding box model coordinates. This demonstrated the effectiveness of the contouring approach. Evaluating additional results on CT scan images with different tumor locations showed the high accuracy and repeatability of the approach.

This validates that the goals were successfully achieved by implementing computer vision algorithms and a contouring methodology in OpenCV. Segmentation and coordinated determination of tumors from CT scans were made possible. However, the center coordinates obtained from the contouring model created by the author can be further applied to surgical robotic arms, as shown in Figure 38 below, through inverse kinematics. By providing the coordinates of the tumor's center as the target position, inverse kinematics techniques can be applied to mathematically determine the joint configurations required to align the biopsy tool at the tumor. This helps dynamically plan collision-free trajectories for the robotic arm and end effector to accurately approach and position itself at the tumor from various initial arm postures. The joint angles produced by inverse kinematics are then used to smoothly actuate and coordinate the motion of each robotic arm segment along the computed path to the tumor center coordinates. Properly centering the biopsy tool at the tumor coordinates optimized by computer vision ensures a representative tissue sample is collected from the desired target area for effective diagnosis and analysis. Inverse kinematics thus plays a vital role in the precision guidance of the surgical robot for minimally invasive and accurate biopsy procedures under image guidance.

In conclusion, the goal of creating a system to coordinate localization and segment brain tumors was achieved. The center coordinates of brain tumors have been extracted from CT scan pictures by effectively applying computer vision techniques. Even though the initial findings are encouraging, more work must be done before clinical translation. Specifically, they create real-time visual feedback to accommodate intraoperative modifications and enhance the learning model with more datasets. Computer vision has much promise to improve surgical robotic arm control and guidance with further research, increasing the efficacy, safety, and accuracy of image-guided needle biopsy operations.

4.1. Acknowledgements

I wish to express my sincere gratitude to the leadership of Chinhoyi University of Technology (C.U.T.) for allowing me to evolve into a remarkable researcher. My heartfelt thanks extend to all the authors who contributed to this paper; their unwavering support throughout this endeavor is difficult to forget.

4.2. Author contributions

Doubt Simango: Conceptualization, Writing-Original draft preparation, Methodology, Software, Tawanda Mushiri: Data curation, Validation, Abid Yahya: Writing-Reviewing and Editing, Software, Validation. Augustine Ndaimani: Visualization, Investigation, Writing-Reviewing and Editing.

Conflicts of interest

The authors declare no conflicts of interest

References

[1] Yi, S., Liu, S., Xu, X., Wang, X. V., Yan, S., & Wang, L. (2022). A vision-based human-robot collaborative system for digital twins. *Procedia CIRP, 107*(March), 552–557. https://doi.org/10.1016/j.procir.2022.05.024

[2] Zhang, X., Liu, Y., Branson, D. T., Yang, C., Dai, J. S., & Kang, R.(2022). Variable-gain control for continuum robots based on velocity sensitivity. *Mechanismand MachineTheory, 168* (November 2021), 104618. https://doi.org/10.1016/j.mechmachtheory.2021.104618

[3] Thenuwara, G., Curtin, J., & Tian, F. (2023). Advances in Diagnostic Tools and Therapeutic Approaches for Gliomas: A Comprehensive Review. Sensors, 23(24), 1–47. https://doi.org/10.3390/s23249842

[4] Saha, M., Mukherjee, R., & Chakraborty, C. (2016). Computer-aided diagnosis of breast cancer using cytological images: A systematic review. Tissue and Cell, 48(5), 461–474. https://doi.org/10.1016/j.tice.2016.07.006

[5] Pulumati, A., Pulumati, A., Dwarakanath, B. S., Verma, A., & Papineni, R. V. L. (2023). Technological advancements in cancer diagnostics: Improvements and limitations. Cancer Reports, 6(2), 1– 17. https://doi.org/10.1002/cnr2.1764

[6] Zhang, F., Jin, G., Dai, M., Ding, M., Zhang, J., & Zhang, X. (2023). Percutaneous Magnetic Resonance Imaging-Guided Coaxial Cutting Needle Biopsy of Pancreatic Lesions: Diagnostic Accuracy and Safety. Cardiovascular and Interventional Radiology, 46(11), 1603–1609. https://doi.org/10.1007/s00270-023-03485-z

[7] Han, Z., Yu, K., Hu, L., Li, W., Yang, H., Gan, M., Guo, N., Yang, B., Liu, H., & Wang, Y. (2019). A targeting method for robot-assisted percutaneous needle placement under fluoroscopy guidance. Computer Assisted Surgery, 24(sup1), 44–52. https://doi.org/10.1080/24699322.2018.1557907

[8] Lim, S., Jun, C., Chang, D., Petrisor, D., Han, M., &

[9] Stoianovici, D. (2019). Robotic transrectal ultrasound-guided prostate biopsy. IEEE Transactions on Biomedical Engineering, 66. https://doi.org/10.1109/TBME.2019.2891240

[10] Welleweerd, M. K., Pantelis, D., De Groot, A. G., Siepel, F. J.& Stramigioli, S. (2020). Robot-assisted ultrasound- guidedbiopsy on MR-detected breast lesions. IEEE International Conference on Intelligent Robots and Systems. https://doi.org/10.1109/IROS45743.2020.9341695

[11] Chen, B., Shorey, J., Saunders, R. S., Richard, S., Thompson, J., Nolte, L. W., & Samei, E. (2011). An Anthropomorphic Breast Model for Breast Imaging Simulation and Optimization. Academic Radiology, 18(5). https://doi.org/10.1016/j.acra.2010.11.009

[12] Sajadi, S. M. R., Karbasi, S. M., Brun, H., Tørresen, J., Elle, O. J., & Mathiassen, K. (2022).Towards Autonomous Robotic Biopsy— Design, Modeling and Control of a Robot for Needle Insertion of a Commercial Full Core BiopsyInstrument. Frontiers in Robotics and AI, 9. https://doi.org/10.3389/frobt.2022.896267

[13] Guo, Z., Tai, Y., Du, J., Chen, Z., Li, Q., & Shi, J. (2021). Automatically Addressing System for Ultrasound-Guided Renal Biopsy Training Based on Augmented Reality. IEEE Journal of Biomedical and Health Informatics, 25(5). https://doi.org/10.1109/JBHI.2021.3064308

[14] Hu, Y., Cai, P., Zhang, H., Adilijiang, A., Peng, J., Li, Y., Che, S., Lan, F., & Liu, C. (2022). A Comparation Between Frame- Based and Robot-Assisted in Stereotactic Biopsy. Frontiers in Neurology, 13, 928070. https://doi.org/10.3389/FNEUR.2022.928070/BIBTEX

[15] Takahashi et al., 2022) Takahashi, Y., Izumi, K., Saito, R., Ikeda, I., Tsumura, R., & Iwata, H. (2022). Development of Needle Guide Unit Considering Buckling Bone-Perforation Control Strategy Based on Computed Tomography-Guided Needle Insertion Robot. Proceedings of the Annual International Conference of the IEEE Engineering in Medicine and Biology Society, EMBS, 2022-July, 4391–4396. https://doi.org/10.1109/EMBC48229.2022.9871709

[16] Ben-David, E., Shochat, M., Roth, I., Nissenbaum, I., Sosna, J., & Goldberg, S. N. (2018). Evaluation of a CT-Guided Robotic System for Precise Percutaneous Needle Insertion. Journal of Vascular and Interventional Radiology, 29(10), 1440–1446. https://doi.org/10.1016/J.JVIR.2018.01.002

[17] Nagao, A., Matsuno, T., Kimura, K., Kamegawa, T., Minami, M., & Hiraki, T. (2017). Installation angle offset compensation of puncture robot based on measurement of the needle by CT equipment. 2017 IEEE International Conference on Mechatronics and Automation, ICMA 2017, 451–457. https://doi.org/10.1109/ICMA.2017.8015859

[18] Agarwal, A. (2018). Review of Optical Flow Technique for Moving Object Detection. December 2016. https://doi.org/10.1109/IC3I.2016.7917999

[19] Ahmed, S. F., Alam, S. Bin, Hassan, M., Rozbu, M.

R., Ishtiak, T., Rafa, N., Mofijur, M., Ali, A. B. M. S., & Gandomi, A. H. (2023). Deep learning modelling techniques : current progress , applications , advantages , and challenges. In Artificial Intelligence Review (Vol. 56, Issue 11). Springer Netherlands. https://doi.org/10.1007/s10462-023-10466-8

[20] Simplification, F. D. (2022). applied sciences Research on Image Matching of Improved SIFT Algorithm Based on Stability Factor and Feature Descriptor Simplification.

[21] Hutchinson S., Hager G. D. and Corke P.I., 2006. A tutorial in visual servo control. IEEE Transactions on robotics and automation. Vol. 12, No. 5, p. 65.

[22] Garcia, G., Corrales Ramon, J. A., Pomares, J., & Fernando, T. (2009). Survey of Visual and Force/Tactile Control of Robots for Physical Interaction in Spain. Sensors, 9. https://doi.org/10.3390/s91209689

[23] Chaumette F, Hutchinson S (2006) Visual servo control, part I: basic approaches. IEEE Robot Autom Mag 13(4):82–90

[24] Corke P. I., 2011. Robotics, Vision and Control. Fundamental algorithms in MATLAB. Springer.

[25] Habuza, T., Navaz, A. N., Hashim, F., Alnajjar, F., Zaki, N., Serhani, M. A., & Statsenko, Y. (2021). AI applications in robotics, diagnostic image analysis and precision medicine: Current limitations, future trends, guidelines on CAD systems for medicine. Informatics in Medicine Unlocked, 24,100596. https://doi.org/10.1016/j.imu.2021.100596

[26] Aderibigbe. (2018). No 主観的健康感を中心とした在宅高齢者 における 健康関連指標に関する共分散構造分析 Title. Energies, 6(1), 1–8

[27] http://journals.sagepub.com/doi/10.1177/1120700020921110%0Aht tps://doi.org/10.1016/j.reuma.2018.06.001%0Ahttps://doi.org/10.10 16/j.arth.2018.03.044%0Ahttps://reader.elsevier.com/reader/sd/pii/S 1063458420300078?token=C039B8B13922A2079230DC9AF11A3 33E295FCD8

[28] Bick, U., Trimboli, R. M., Athanasiou, A., Balleyguier, C., Baltzer, P. A. T., Bernathova, M., Borbély, K., Brkljacic, B., Carbonaro, L. A., Clauser, P., Cassano, E., Colin, C., Esen, G., Evans, A., Fallenberg, E. M., Fuchsjaeger, M. H., & Gilbert, F. J. (2020). Image-guided breast biopsy and localisation : recommendations for information to women and referring physicians by the European Society of Breast Imaging.

[29] Encarnacion, C. O., Ali, A., Johnstone, D. W., & Haasler, G. B. (2017). Clinics in Surgery Imaging Modalities and Image Guided Biopsy Techniques for Lung Cancer Staging and Their Staging Implications for Lung Cancer- A Review for the General Surgeon. 2, 2–4.

[30] Jiménez-lópez, E., De, D. S., Reyes-ávila, L. A., Servín, R., Mora-pulido, D., Melendez-campos, J., & López-martínez, A. A. (2021). Modeling of Inverse Kinematic of 3-DoF Robot , Using Unit Quaternions and Artificial Neural Network. January. https://doi.org/10.1017/S0263574720001071

[31] Le, H. B. Q., Lee, S. T., & Munk, P. L. (2010). Image-Guided Musculoskeletal Biopsies. 1(212), 191–198.

[32] Castelli, F., Michieletto, S., & Ghidoni, S. (2017). A machine learning-based visual servoing approach for fast robot control in industrial setting. December, 1–10. https://doi.org/10.1177/1729881417738884

[33] Siepel, F. J., Maris, B., Welleweerd, M. K., Groenhuis, V., Fiorini, P., & Stramigioli, S. (2021). Needle and Biopsy Robots : a Review. 73–84.

[34] Raza, S., Chikarmane, S. A., Gombos, E. C., Georgian-Smith, D., & Frost, E. P. (2018). Optimizing Success and Avoiding Mishaps in the Most Difficult Image-guided Breast Biopsies. Seminars in Ultrasound, CT and MRI, 39(1), 80–97. https://doi.org/10.1053/j.sult.2017.08.006

[35] Lingegowda, D., Gupta, B., Gehani, A., Sen, S., & Ghosh, P. (2022). Optimization of the Lung Biopsy Procedure : A Primer. 190–201.

[36] Huang, S., Lou, C., Zhou, Y., He, Z., Jin, X., Feng, Y., & Gao, A. (2023). MRI - guided robot intervention — current state - of - the -art and new challenges. In Med-X. Springer Nature Singapore. https://doi.org/10.1007/s44258-023-00003-1

[37] Wang, T., Li, H., Pu, T., & Yang, L. (2023). Microsurgery Robots : Applications , Design , and Development. 1–49.

[38] Shetty, R., Sreekar, H., Lamba, S., & Gupta, A. K. (2012). A novel and accurate technique of photographic wound measurement. Indian Journal of Plastic Surgery, 45(2), 425–429. https://doi.org/10.4103/0970-0358.101333

[39] Cheng, K., Li, L., Du, Y., Wang, J., Chen, Z., Liu, J., Zhang, X., Dong, L., Shen, Y., & Yang, Z. (2023). A systematic review of image-guided, surgical robot-assisted percutaneous puncture: Challenges and benefits. Mathematical Biosciences and Engineering, 20(5), 8375–8399. https://doi.org/10.3934/mbe.2023367

[40] Zhang, Y., Yuan, Q., Muzzammil, H. M., Gao, G., & Xu, Y. (2023). Image-guided prostate biopsy robots:

A review. Mathematical Biosciences and Engineering, 20(8), 15135–15166. https://doi.org/10.3934/mbe.2023678

[41] Klimberg, V. S., & Rivere, A. (2016). Ultrasound image-guided core biopsy of the breast. Chinese Clinical Oncology, 5(3), 1–9. https://doi.org/10.21037/cco.2016.04.05

[42] Welleweerd, M. K., Siepel, F. J., Groenhuis, V., Veltman, J., & Stramigioli, S. (2020). Design of an end-effector for robot-assisted ultrasound-guided breast biopsies. International Journal of Computer Assisted Radiology and Surgery, 15(4), 681–690. https://doi.org/10.1007/s11548-020-02122-1

[43] Hernandez-Guedes, A., Arteaga-Marrero, N., Villa, E., Callico, G. M., & Ruiz-Alzola, J. (2023). Feature Ranking by Variational Dropout for Classification Using Thermograms from Diabetic Foot Ulcers. Sensors, 23(2), 1–18.

[44] Liu, Y., Wu, X., Sang, Y., Zhao, C., Wang, Y., Shi, B., & Fan, Y. (2024). Evolution of Surgical Robot Systems Enhanced by Artificial Intelligence: A Review. Advanced Intelligent Systems. https://doi.org/10.1002/aisy.202300268

[45] Sun, B., Li, D., Song, B., Li, S., Li, C., Qian, C., Lu, Q., & Wang, X. (2023). An Overview of Minimally Invasive Surgery Robots from the Perspective of Human–Computer Interaction Design. Applied Sciences (Switzerland), 13(15). https://doi.org/10.3390/app13158872

[46] Unger, M., Berger, J., & Melzer, A. (2021). Robot-Assisted Image-Guided Interventions. Frontiers in Robotics and AI, 8(July), 1–7. https://doi.org/10.3389/frobt.2021.664622

[47] Sajadi, S. M. R., Karbasi, S. M., Brun, H., Tørresen, J., Elle, O. J., & Mathiassen, K. (2022). Towards Autonomous Robotic Biopsy— Design, Modeling and Control of a Robot for Needle Insertion of a Commercial Full Core Biopsy Instrument. Frontiers in Robotics and AI, 9(June), 1–16. https://doi.org/10.3389/frobt.2022.896267

[48] Xiong, R., Zhang, S., Gan, Z., Qi, Z., Liu, M., Xu, X., Wang, Q., Zhang, J., Li, F., & Chen, X. (2022). A novel 3D-vision–based collaborative robot as a scope holding system for port surgery: a technical feasibility study. Neurosurgical Focus, 52(1), 1–8. https://doi.org/10.3171/2021.10.FOCUS21484